Published in final edited form as:
Oral Dis. 2011 May ; 17(4): 427–432. doi:10.1111/j.1601-0825.2010.01772.x.

Anatomic Site Variability in Rat Skeletal Uptake and Desorption Of Fluorescently Labeled Bisphosphonate

D. Wen[1], **L. Qing**[2,§], **G. Harrison**[3], **E. Golub**[3], and **S.O. Akintoye**[1,*]

[1] Department of Oral Medicine, School of Dental Medicine, University of Pennsylvania, Philadelphia PA

[2] Department of Periodontology & Oral Medicine, School of Stomatology, The Fourth Military Medical University, Xi'an, China

[3] Department of Biochemistry, School of Dental Medicine, University of Pennsylvania, Philadelphia PA

Abstract

Objectives—Bisphosphonates commonly used to treat osteoporosis, Paget's disease, multiple myeloma, hypercalcemia of malignancy and osteolytic lesions of cancer metastasis have been associated with bisphosphonate-associated jaw osteonecrosis (BJON). The underlying pathogenesis of BJON is unclear, but disproportionate bisphosphonate concentration in the jaw has been proposed as one potential etiological factor. This study tested the hypothesis that skeletal biodistribution of intravenous bisphosphonate is anatomic site-dependent in a rat model system.

Materials and Methods—Fluorescently labeled pamidronate was injected intravenously in athymic rats of equal weights followed by *in vivo* whole body fluorimetry, *ex vivo* optical imaging of oral, axial and appendicular bones and ethylenediaminetetraacetic acid bone decalcification to assess hydroxyapatite-bound bisphosphonate.

Results—Bisphosphonate uptake and bisphosphonate released per unit calcium were similar in oral and appendicular bones but lower than those in axial bones. Hydroxyapatite-bound bisphosphonate liberated by sequential acid decalcification was highest in oral relative to axial and appendicular bones ($p < 0.05$).

Conclusions—This study demonstrates regional differences in uptake and release of bisphosphonate from oral, axial and appendicular bones of immune deficient rats.

Keywords

Bisphosphonate; osteonecrosis; jaw; fluorescent labeling; bone

Introduction

Bisphosphonates (BPs) are efficacious in the treatment of osteoporosis, Paget's disease, multiple myeloma, hypercalcemia of malignancy and osteolytic lesions of cancer metastasis. However several nitrogen-containing bisphosphonates are associated with spontaneous jaw necrosis (Migliorati et al., 2006, Ruggiero et al., 2006, Woo et al., 2006). While

[*]Please address all correspondence to: Sunday O. Akintoye BDS, DDS, MS, University of Pennsylvania, School of Dental Medicine, Department of Oral Medicine, The Robert Schattner Center Room 211, 240 South 40th Street, Philadelphia PA 19104, Phone: 215-898-9932, Fax: 215-573-7853, akintoye@dental.upenn.edu.
[§]Visiting Scholar, Department of Oral Medicine, School of Dental Medicine, University of Pennsylvania, Philadelphia PA

bisphosphonate-associated jaw osteonecrosis (BJON) is clinically similar to osteoradionecrosis (ORN) based on characteristic tissue dehiscence, chronic bone devitalization and lytic radiographic features, the underlying pathogenesis of BJON is still unclear (Sarin et al., 2008).

Bisphosphonates are analogues of pyrophosphate with oxygen substituted with carbon in the pyrophosphate bond to form a phosphate-carbon-phosphate (P-C-P) structural backbone. Selective modification of sides chains attached to the carbon atom has produced bisphosphonates with distinct physicochemical and biological characteristics as well as enhanced binding affinity and anti-resorptive properties (Rodan & Fleisch, 1996). Avid binding of bisphosphonates to hydroxyapatite keep them unmetabolized for long periods of time (Jung et al., 1973, Fleisch, 1998). This remarkable physicochemical property is due to binding of the phosphate ends of bisphosphonate to metal ions, including calcium to form both soluble and insoluble complexes and the resistance of their P-C-P structural backbone to heat, most chemicals and enzymatic hydrolysis (Fleisch, 2000). Specifically, the strong association of intravenous nitrogen-containing bisphosphonates with BJON relative to oral formulations suggests that intravenous administration enhances higher bisphosphonate bioavailability. About 50% of intravenous bisphosphonates is bioavailable for incorporation into bone matrix compared to an average of 1% of oral bisphosphonates due to delayed gastrointestinal tract absorption (Ezra & Golomb, 2000).

It is still unclear why bisphosphonate-associated osteonecrosis is limited to the jaws. Suggested theories focus on local factors unique to orofacial bones in health and disease (Sarin et al., 2008, Stefanik et al., 2008, Stefanik et al., 2006), but existence of skeletal site-disparity in biodistribution and bioavailability of bisphosphonates is yet to be fully clarified. Additionally, it is unclear if bisphosphonates are disparately sequestered in orofacial bones based on differential uptake and release of hydroxyapatite-bound bisphosphonate. The premise is that higher orofacial bone uptake of bisphosphonate may potentially reach concentrations high enough to become toxic to oral epithelium and alter normal oral tissue healing. The present study used fluorescently tagged pamidronate (a nitrogen-containing bisphosphonate strongly associated with BJON) to test the hypothesis that skeletal uptake and release of bisphosphonate in rats is anatomic site-dependent. We demonstrated in immunodeficient rats, regional differences in skeletal uptake and release of bisphosphonate in oral, axial and appendicular bones but implications for site-selectivity of BJON and effects of immune modulation need further clarifications.

Materials and Methods

Study animals

Four female 250 g athymic rats (NIH-RNU-F nude rats, Taconic Farms, Germantown NY) were given intravenous bisphosphonate under animal protocol (# 801312) approved by University of Pennsylvania Office of Regulatory Affairs.

In vivo imaging of fluorescently tagged bisphosphonate

Animals were anesthetized with parenterally administered cocktail of ketamine (37 mg/kg body weight) and medetomidine (0.5 mg/kg body weight). Following manufacturer's recommendation, each animal received tail vein injection of 80 nmol/kg body weight of far red fluorescently-tagged pamidronate (OsteoSense ™680, Cat # 10020, VisEn Medical, Woburn, MA) in 150 μl phosphate buffered saline (PBS). Anesthesia was immediately reversed with antipamezole (1mg/kg body weight). Twenty four hours after bisphosphonate injection, animals were re-anesthetized, residual skin hair was shaved and images of hydroxyapatite-bound bisphosphonate was acquired with an optical imager (Maestro ™, CRI

Inc, Woburn, MA) using deep red filters (excitation range 671–705 nm, emission of 750 nm long pass). Animals were positioned to capture images of upper and lower one half of the body from ventral and dorsal views before they were sacrificed by CO_2 asphyxiation. Individual bone parts were immediately dissected free of soft tissues, shielded from light and stored at −20°C. Using similar *in vivo* imaging parameters, bone parts were scanned a second time before desorption of bound bisphosphonate (Figure 1). Bisphosphonate signal intensity in the images were analyzed with ImageJ (version, 1.40G, National Institutes of Health, Bethesda MD) after defining specific regions of interest (ROI) that correlate with bone sections subsequently recovered for desorption of bound bisphosphonate (as described below). Bisphosphonate signal intensity per unit area normalized to adjacent background intensity was expressed as relative fluorescence units (RFU).

Desorption of hydroxyapatite-bound bisphosphonate

Bone parts were grouped into three anatomic regions: oral (mandible), appendicular (humerus, radius/ulnar, femur, tibia/fibula) and axial (ribs, vertebrae) for comparative analysis of bisphosphonate uptake. Left and right mandibles were analyzed separately after removing attached teeth. Similarly, bone sections of comparatively equal weight as mandible were analyzed from long bone diaphysis, ribs and vertebrae. Serial decalcification to remove calcium-bound bisphosphonate was achieved with 0.5 M ethylenediaminetetraacetic acid (EDTA), pH 8.0 at 37°C in the dark using a rotary shaker. The EDTA solution was changed twice so that released calcium and bisphosphonate were recovered after 24, 48 and 120 hours of consecutive decalcification (Figure 1). Recovered fluorescently-tagged bisphosphonate was measured with a Fluorometer (Photon Technology International, Birmingham, NJ) at wavelengths of 695 nm excitation and 700–705 nm emission while calcium released in solution was measured with an Atomic Absorption Spectrophotometer (PerkinElmer, Waltham, MA) at wavelength of 422.7nm. Absolute amounts of bisphosphonate and calcium were computed from respective standard curves.

Statistical Analysis

Mean RFU was used to assess hydroxyapatite-associated fluorescence *in vivo*. Mean site-specific RFU was correlated with respective bisphosphonate and calcium amounts from corresponding bone sections. Anatomic site differences of ROIs were analyzed and compared based on oral, axial and appendicular regions. Data was expressed as mean ± standard deviation, analyzed by one-way analysis of variance (ANOVA) followed by Dunn-Sidak post hoc multiple comparisons with SigmaStat 3.1 statistical package (Systat Software, Chicago, IL, USA). Statistical significance was set at $p < 0.05$.

Results

Athymic rats were selected based on their nude skin since hair interferes with optical imaging. Each rat received a metabolic dose of 60.7 μg/kg body weight bisphosphonate (Table 1) which is approximately 4.3 mg pamidronate. Fluorescence intensity of hydroxyapatite-bound bisphosphonate in all animals was regionally variable and stronger than adjacent soft tissues (Figures 2A). All the bone parts demonstrated heterogeneous labeling. There was relatively higher signal intensity in the mandibular condyle than the relatively more homogeneous intensity in the body of mandible (Figure 2B). Similarly, there was higher labeling intensity at proximal and distal ends of the long bones (Figure 2C), anterior ends of the rib cage and intervertebral discs (Figure 2D). Total bisphosphonate signal intensity in oral bone was similar to that of appendicular bone but lower than that of axial bone (Figure 2E). Sequential and cumulative amounts of bisphosphonate released from bone sections after three rounds of decalcification indicate significantly higher hydroxyapatite-bound bisphosphonate ($p < 0.05$) in oral bones relative to axial and

appendicular sites (Figures 3A and B). Interestingly, extractable bisphosphonate from oral bones after 120 hours was still relatively higher than bisphosphonate extractable from either axial or appendicular bones even at the initial 24 hour-time point (Figures 3A and B). As expected, these regional differences were consistent with calcium serially released from the different anatomic regions (Figure 3C and D) since bisphosphonate binds to hydroxyapatite. Consistent with bisphosphonate signal intensity in Figure 2E, the amount of bisphosphonate per unit calcium released in oral and appendicular bones were similar but lower than axial bone (Figure 3E).

Discussion

BJON is an established oral complication associated with long-term treatment with nitrogen-containing bisphosphonate (Marx et al., 2005, Migliorati et al., 2005, Woo et al., 2006). Pathogenesis of BJON is still unclear, but proposed theories include a relatively higher concentration of bisphosphonate in the jaws, enhanced bisphosphonate anti-osteoclastic and anti-angiogenesis actions, possible uncoupling of osteoblast-osteoclast equilibrium and a combination of drug, patient and oral issues acting in concert to produce a ‘band-wagon effect’ (Sarin et al., 2008, Reid et al., 2007). To further clarify preferential bisphosphonate concentration in the jaws, we tested and evaluated biodistribution and bioavailability of fluorescently tagged pamidronate strongly associated with BJON because of its high affinity for hydroxyapatite and high anti-resorptive actions. High binding affinity and immediate skeletal binding of single doses of bisphosphonate is saturable, so that unbound drug is rapidly eliminated by renal clearance (Rogers, 2003). About 56–66% of bisphosphonate is retained in the skeleton within the first 6 hours (Lin et al., 1992), (Zaheer et al., 2001), so we used fluorescently tagged pamidronate evaluable as early as 2 hours post-injection and performed optical imaging at 24 hours to allow for adequate bisphosphonate biodistribution as well as elimination of unbound drug.

Bisphosphonate is purported to concentrate in the jaws hundred times more than other skeletal sites (Reid et al., 2007) possibly due to unique jaw bone architecture or vascularity; our data support regional differences and heterogeneous skeletal affinity for bisphosphonate based on whole body fluorimetry in this rat model. Higher bisphosphonate signal intensity displayed by axial bone (Figure 2E) is apparently size-dependent because the vertebral bones are larger and demonstrated higher bisphosphonate per unit calcium than oral and appendicular bones (Figure 3E). But the quantitatively higher bisphosphonate released from oral bone may be related to higher hydroxyapatite content (Figures 3B and 3D) that translates into higher jaw bone affinity for bisphosphonate. Thus, our results support assertions that mandible is structurally denser than axial and appendicular bones and display higher skeletal bisphosphonate uptake.

Bisphosphonate skeletal accumulation is also influenced by rate of liberation from bone. Bone with higher remodeling ability preferentially accumulates more bisphosphonate due to greater amount of actively resorbing surface that favors bisphosphonate binding (Bauss et al., 2002, Sato et al., 1991). However hydroxyapatite-bound bisphosphonate is also continuously liberated in rapidly remodeling bone owing to the locally acidic environment produced by osteoclasts (Sato et al., 1991). Also sites with high remodeling activity have greater metabolic demands and higher blood flow that favor rapid elimination of bisphosphonate. Our analysis of oral, axial and appendicular bones supports site-disparity in bisphosphonate dissociation. It showed clearly that bisphosphonate was readily liberated mostly from the jaw bones (Figure 3) supporting the theory of higher jaw bone remodeling relative to non-oral sites (Huja et al., 2006). Therefore, a potentially more rapid release of jaw-bound bisphosphonate translates to reduced bisphosphonate therapeutic efficacy in the jaws. Consequent reduction in bisphosphonate anti-resorptive action can predispose jaw

bones to higher osteoclast mediated bone resorption. Pamidronate has also been shown to be more toxic to jaw osteoprogenitor cells (Stefanik et al., 2008), so rise in osteoclast recruitment combined with reduction in number of osteoprogenitor cells will uncouple osteoblast-osteoclast balance (Sarin et al., 2008). An increase in jaw bone resorption without compensatory bone formation favors regional bone death. Prior exposure of jaw bone to bisphosphonate also supports progression of BJON since high bisphosphonate concentration causes direct toxicity to osteocytes, osteoblasts and osteogenic precursors (Idris et al., 2008, Stefanik et al., 2008, Stefanik et al., 2006). Therefore, focal loss of osteocytes and canaliculi network (Allen & Burr, 2008, Hansen et al., 2006) can promote accumulation of regions of dead osteocytes and non-viable bone over time (Allen, 2009a).

The limitations of this pilot study must be noted. Nude skin of athymic rats minimizes interference with optical imaging but assessing the added effects of immune surveillance was not practicable in athymic rats. Pamidronate metabolic dose of 60.7 μg/kg body weight is less than human doses (Allen, 2009b, Fuchs et al., 2008), but it is clinically relevant considering that serum concentration of pamidronate is 2.5 μg/ml 4 hours after infusion [(Stefanik et al., 2008); United States Package Insert; Novartis Pharmaceuticals]. Notwithstanding, a dose of bisphosphonate that is 30 times less than human doses has been associated with jaw osteonecrosis in another rat model (Allen, 2009b, Sonis et al., 2009). An earlier study evaluated subcutaneously administered ibandronate in a single rat but reported no site differences in ibandronate uptake (Bauss et al., 2008); the current study advanced our understanding of site-disparity in skeletal uptake and release of bisphosphonate using four, although limited, number of athymic rats. Future work in immunocompetent animals will further clarify the roles of immune surveillance in the initiation of BJON. Additionally, optical imaging modality supports acquisition of two-dimensional planar images with limited anatomical detail compared to structural imaging modalities like micro-computed tomography (micro-CT). However, future evaluation of site differences with three-dimensional optical tomography, micro-CT and histological evaluation of depth of bisphosphonate penetration will provide more structural detail of hydroxyapatite-bound bisphosphonate. This study did not assess the whole skeleton; also teeth, proximal and distal ends of long bones were excluded to minimize confounding effects. Finally, serial decalcification with EDTA is a simulation of locally acidic environment in osteoclast-mediated bone resorption and analysis of calcium-bound bisphosphonate is an indirect assessment of hydroxyapatite-bound bisphosphonate. Therefore, further studies using larger samples and more specialized equipments will give additional insights on the impact of disproportionate regional bisphosphonate skeletal uptake and liberation on the pathogenesis of BJON.

Acknowledgments

We thank Drs. Arthur Kuperstein and Yvette Liu for technical assistance and Dr. Faizan Alawi for useful comments. This project was supported in part with funds from Penn Center for Musculoskeletal Disorders funded by NIH/NIAMS research grant AR050950, University of Pennsylvania Research Foundation and USPHS/NIH/NCI research grant 5K08CA120875-03.

References

Allen MR. Bisphosphonates and osteonecrosis of the jaw: moving from the bedside to the bench. Cells Tissues Organs. 2009a; 189:289–94. [PubMed: 18698128]

Allen MR. Does Rat + Bisphosphonate + Exposed Bone = An Animal Model of ONJ? IBMS BoneKEy. 2009 Jun 1. 2009b. 10.1138/20090383IBMS BoneKEy. International Bone & Mineral Society; Washington, DC: 2009 Jun 1. p. 227-231.Edition

Allen MR, Burr DB. Mandible matrix necrosis in beagle dogs after 3 years of daily oral bisphosphonate treatment. J Oral Maxillofac Surg. 2008; 66:987–94. [PubMed: 18423290]

Bauss F, Lalla S, Endele R, Hothorn LA. Effects of treatment with ibandronate on bone mass, architecture, biomechanical properties, and bone concentration of ibandronate in ovariectomized aged rats. J Rheumatol. 2002; 29:2200–8. [PubMed: 12375334]

Bauss F, Pfister T, Papapoulos S. Ibandronate uptake in the jaw is similar to long bones and vertebrae in the rat. J Bone Miner Metab. 2008; 26:406–8. [PubMed: 18600409]

Ezra A, Golomb G. Administration routes and delivery systems of bisphosphonates for the treatment of bone resorption. Adv Drug Deliv Rev. 2000; 42:175–95. [PubMed: 10963835]

Fleisch H. Bisphosphonates: mechanisms of action. Endocr Rev. 1998; 19:80–100. [PubMed: 9494781]

Fleisch, H. Bisphosphonates in bone disease: From the laboratory to the patient. Academic Press; San Diego: 2000.

Fuchs RK, Allen MR, Condon KW, Reinwald S, Miller LM, McClenathan D, Keck B, Phipps RJ, Burr DB. Calculating clinically relevant drug doses to use in animal studies. Osteoporosis International. 2008; 19:1815–1817.

Hansen T, Kunkel M, Weber A, James Kirkpatrick C. Osteonecrosis of the jaws in patients treated with bisphosphonates - histomorphologic analysis in comparison with infected osteoradionecrosis. J Oral Pathol Med. 2006; 35:155–60. [PubMed: 16454811]

Huja SS, Fernandez SA, Hill KJ, Li Y. Remodeling dynamics in the alveolar process in skeletally mature dogs. Anat Rec A Discov Mol Cell Evol Biol. 2006; 288:1243–9. [PubMed: 17075846]

Idris AI, Rojas J, Greig IR, Van't Hof RJ, Ralston SH. Aminobisphosphonates cause osteoblast apoptosis and inhibit bone nodule formation in vitro. Calcif Tissue Int. 2008; 82:191–201. [PubMed: 18259679]

Jung A, Bisaz S, Bartholdi P, Fleisch H. Influence of pyrophosphate on the exchange of calcium and phosphate ions on hydroxyapatite. Calcif Tissue Res. 1973; 13:27–40. [PubMed: 4356313]

Lin JH, Chen IW, Duggan DE. Effects of dose, sex, and age on the disposition of alendronate, a potent antiosteolytic bisphosphonate, in rats. Drug Metab Dispos. 1992; 20:473–8. [PubMed: 1356720]

Marx RE, Sawatari Y, Fortin M, Broumand V. Bisphosphonate-induced exposed bone (osteonecrosis/osteopetrosis) of the jaws: risk factors, recognition, prevention, and treatment. J Oral Maxillofac Surg. 2005; 63:1567–75. [PubMed: 16243172]

Migliorati CA, Schubert MM, Peterson DE, Seneda LM. Bisphosphonate-associated osteonecrosis of mandibular and maxillary bone: an emerging oral complication of supportive cancer therapy. Cancer. 2005; 104:83–93. [PubMed: 15929121]

Migliorati CA, Siegel MA, Elting LS. Bisphosphonate-associated osteonecrosis: a long-term complication of bisphosphonate treatment. Lancet Oncol. 2006; 7:508–14. [PubMed: 16750501]

Reid IR, Bolland MJ, Grey AB. Is bisphosphonate-associated osteonecrosis of the jaw caused by soft tissue toxicity? Bone. 2007; 41:318–20. [PubMed: 17572168]

Rodan GA, Fleisch HA. Bisphosphonates: mechanisms of action. J Clin Invest. 1996; 97:2692–6. [PubMed: 8675678]

Rogers MJ. New insights into the molecular mechanisms of action of bisphosphonates. Curr Pharm Des. 2003; 9:2643–58. [PubMed: 14529538]

Ruggiero SL, Fantasia J, Carlson E. Bisphosphonate-related osteonecrosis of the jaw: background and guidelines for diagnosis, staging and management. Oral Surg Oral Med Oral Pathol Oral Radiol Endod. 2006; 102:433–41. [PubMed: 16997108]

Sarin J, DeRossi SS, Akintoye SO. Updates on bisphosphonates and potential pathobiology of bisphosphonate-induced jaw osteonecrosis. Oral Dis. 2008; 14:277–85. [PubMed: 18336375]

Sato M, Grasser W, Endo N, Akins R, Simmons H, Thompson DD, Golub E, Rodan GA. Bisphosphonate action. Alendronate localization in rat bone and effects on osteoclast ultrastructure. J Clin Invest. 1991; 88:2095–105. [PubMed: 1661297]

Sonis ST, Watkins BA, Lyng GD, Lerman MA, Anderson KC. Bony changes in the jaws of rats treated with zoledronic acid and dexamethasone before dental extractions mimic bisphosphonate-related osteonecrosis in cancer patients. Oral Oncol. 2009; 45:164–72. [PubMed: 18715819]

Stefanik D, Sarin J, Lam T, Levin L, Leboy PS, Akintoye SO. Disparate osteogenic response of mandible and iliac crest bone marrow stromal cells to pamidronate. Oral Dis. 2008; 14:465–71. [PubMed: 18938273]

Stefanik D, Sarin J, Vogell A, Levin L, Leboy PS, Akintoye SO. Effects of pamidronate on oro-facial human bone marrow stromal cells. J Dent Res. 2006; 85:430.

Woo SB, Hellstein JW, Kalmar JR. Narrative [corrected] review: bisphosphonates and osteonecrosis of the jaws. Ann Intern Med. 2006; 144:753–61. [PubMed: 16702591]

Zaheer A, Lenkinski RE, Mahmood A, Jones AG, Cantley LC, Frangioni JV. In vivo near-infrared fluorescence imaging of osteoblastic activity. Nat Biotechnol. 2001; 19:1148–54. [PubMed: 11731784]

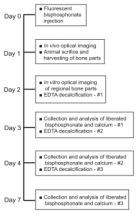

Figure 1.
Experimental outline

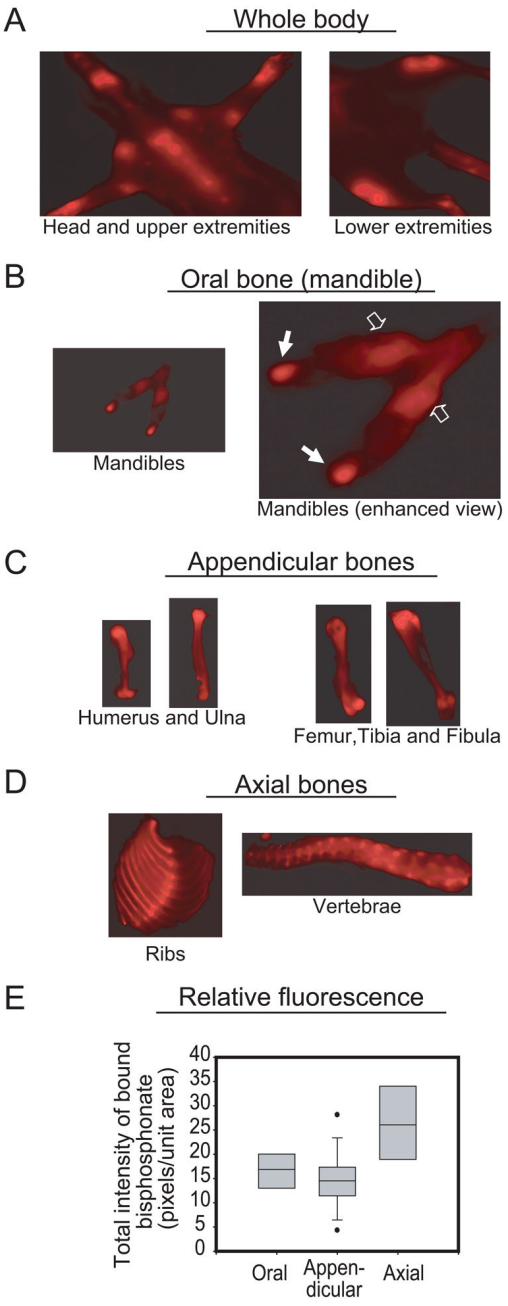

Figure 2.

In vivo optical imaging of hydroxyapatite-bound bisphosphonate. Representative ventral view of the whole body of a rat (A) showing signal intensity of regional skeletal uptake of fluorescently labeled bisphosphonate. Following dissection, representative *in vitro* images demonstrated variable bisphosphonate skeletal uptake. The mandible [oral bone] was displayed strong intensity in the body (B, clear arrows) and condyles (B, solid arrows). Similarly, signal intensity was stronger in the proximal and distal ends relative to the diaphysis of the long bones [appendicular bones] (C). Signal intensity was heterogeneous in the ribs and vertebra [axial bones] (D). Analysis of regional signal intensity in the animals showed variable skeletal uptake as presented in the box and whisker plots (E) [n = 4; median

is the line within the box; the ends of the boxes define 25th and 75th percentiles; the two bars outside the box define 10th and 90th percentiles].

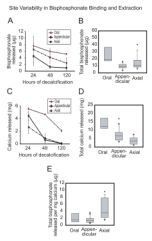

Figure 3.

Regional variability in skeletal uptake and release of fluorescently labeled bisphosphonate. Time-dependent release of hydroxyapatite-bound bisphosphonate (A) and calcium (C) as well as total bisphosphonate (B) and calcium (D) released were significantly highest in oral bones relative to axial and appendicular sites ($p < 0.05$); an indication that bisphosphonate can be readily liberated from the mandible due to the ease of calcium release. Bisphosphonate per unit calcium (E) was highest in axial bone relative to oral and appendicular bones [n = 4; median is the line within the box; the ends of the boxes define 25th and 75th percentiles; the two bars outside the box define 10th and 90th percentiles].

Table 1

Calculation of metabolic dose of pamidronate injected in rats relative to human dose of 60 mg pamidronate (Allen, 2009b, Fuchs et al., 2008)

Rat pamidronate metabolic dose relative to humans*	Rat	Human	
Body weight (Kg)	0.25	60	70
Metabolic weight (kg) = [actual weight]$^{0.75}$	0.354	22	24.2
Drug dose injected (μg/kg body weight)	86	1000	857.1
Actual dose (μg) = dose/[1/body weight]	21.5	60000	5999.7
Metabolic dose (μg/kg) = actual dose/metabolic weight)	60.7	2727.3	2479.2

*Calculations based on rat dose of 80 nmol/kg body weight and 60 mg dose in humans (Allen, R.W. 2009: Fuchs, R.K. 2008)